JMEPEG (2011) 20:671–678
DOI: 10.1007/s11665-010-9814-y

1059-9495/$19.00

Biomechanical Study of Acetabular Tridimensional Memoryalloy Fixation System

Xin-Wei Liu, Shuo-Gui Xu, Yun-Tong Zhang, and Chun-Cai Zhang

(Submitted April 10, 2010; in revised form October 7, 2010)

We developed the acetabular tridimensional memoryalloy fixation system (ATMFS), which is made of NiTi shape memory alloy, according to the specific mechanical properties of biological memory material, NiTi shape memory alloy and measured distribution of contact area and pressure between the acetabulum and the femoral head of cadaveric pelvis. Seven formalin-preserved cadaveric pelves were used for this investigation. Pressure-sensitive film was used to measure contact area and pressure within the anterior, superior, and posterior regions of the acetabulum. The pelves were loaded under the following four conditions: (1) intact; (2) following a creation posterior wall fracture defect; (3) following reduction and standard internal fixation with reconstruction plate; and (4) following reduction and internal fixation with a new shape memory alloy device named ATMFS. A posterior wall fracture was created along an arc of 40° to 90° about the acetabulur rim. Creation of a posterior wall defect resulted in increased load in the superior acetabulum (1485 N) as compared to the intact condition (748 N, $P = 0.009$). Following reduction and internal fixation, the load distributed to the superior acetabulum (1545 N) was not statistically different from the defect condition. Following the fixation with ATMFS, the load seen at the superior region of the actabulum (964 N) was familiar with fixation with reconstruction plate and was not different from intact state ($P = 0.45$). These data indicate that the use of ATMFS as a fracture internal fixation device resulted a partial restoration of joint loading parameters toward the intact state. ATMFS fixation may result in a clinical benefit.

Keywords acetabular tridimensional memoryalloy fixation system, acetabulum, biomechanics, fracture, Ni-Ti alloy

1. Introduction

In 1963, Buehler and Wang (Ref 1) from the American Naval Weapon Research Institute reported on the apparent shape memory effect of NiTi shape memory alloy that aroused widespread interest from relevant scholars. NiTi shape memory alloy, with the effect of shape memory and its superiority in wear and corrosion resistance (Ref 2), has been extensively applied in the medical field (Ref 3) and is considered to be a rare "bio-memory material." Biocompatibility studies have shown NiTi shape memory alloy to be a safe implant material (Ref 4, 5). The NiTi hemofilter designed by Simon was demonstrated to be effective following application in 147 patients at 19 cardiovascular centers (Ref 6). Later on, with further studies, shape memory alloys were gradually applied in clinical practices such as the department of stomatology or orthopedics, and gained huge success (Ref 6-8).

Fractures of the posterior wall are the most common of the acetabular fractures (Ref 9, 10). Operative treatment of these fractures has produced varying results by different authors (Ref 11, 12). One of the major goals in managing acetabular fractures is the prevention of posttraumatic arthritis. Unreduced fractures involving the weightbearing portion of the acetabulum lead to arthritis (Ref 8). When fractures occur in the acetabulum, loading is significantly altered throughout the hip (Ref 13, 14). These alterations in loading were observed even after a simulated posterior wall fracture is reduced and fixed anatomically with standard buttress plating techniques, as previously described (Ref 15, 16). Posttraumatic hip arthritis has been reported in association with as many as 20% of posterior wall acetabular fractures treated with open reduction and internal fixation (Ref 17). It has been postulated that increased joint contact stresses from incongruity or altered load distributions within the hip joint eventually leads to degenerative posttraumatic arthritis through repetitive cartilage damage (Ref 16, 18). Thus, improving articular fragment stabilization beyond that attainable with standard internal fixation techniques may result in decreased fragment motion and therefore improved load distribution.

The bones of pelvis have a structure similar to sandwich, which composed of cortical bone-cancellous bone-cortical bone. Pelvic bones have lower elastic modulus compared with limb bones which composed of cortical bone only. Fracture fixation device made of nickel titanium shape memory alloy with lower elastic modulus will be more beneficial to fracture healing (Ref 19). We developed the acetabular tridimensional memory alloy-fixation system (ATMFS), which is made of NiTi shape memory alloy and patented in China (No. ZL 01 3 52647.2), according to the specific mechanical properties of

This article is an invited paper selected from presentations at Shape Memory and Superelastic Technologies 2010, held May 16-20, 2010, in Pacific Grove, California, and has been expanded from the original presentation.

Xin-Wei Liu, Shuo-Gui Xu, Yun-Tong Zhang, and **Chun-Cai Zhang**, Department of Orthopaedic Surgery, Changhai Hospital, The Second Military Medical University, Shanghai 200433, China. Contact e-mail: bonexu@yahoo.cn.

NiTi shape memory alloy and the anatomical and biomechanical features of acetabulum (Ref 20, 21). Current accepted internal fixation methods include interfragmentary screws and a buttress plate to counteract force applied via the femoral head. The use of ATMFS as a new method to posterior wall fracture fixation has not yet been evaluated. To test the hypothesis that operative reduction and internal fixation of a fracture of the posterior wall of the acetabulum with the use of ATMFS or plate will restore normal mechanical function to the joint, we examined the mechanics of load transfer on intact, fractured, repaired acetabula with ATMFS or plate.

2. Experimental Procedure

2.1 Specimens

Considering the problem of osteoporosis of female specimens, we only selected male specimens in this investigation. Seven complete human pelvis which were including the forth lumbar vertebra and proximal 1/3 femoral shaft were obtained from the formalin-preserved cadavers of seven adult males, without known metabolic bone disease or tumors. Only one hip was used for testing from each hip surgery. The specimens were harvested with a layer of periosteum and muscle insertions intact and with all ligaments and capsules of both hip joints intact. Mean age at the time of death was 65 years (ranged 45-76 years). The trabecular appearance and bony quality were examined and bone abnormalities were ruled out by a standard anteroposterior x-ray. Soft tissue was removed, except ligaments of the sacro-iliac joint and pubic symphysis.

The specimen was fixed in the position of double-limb stance (Fig. 1a), as previously described by Sawaguchi et al. (Ref 22). The specimen was placed in a specific neutral position defined with the iliac wings level (coplanar in the horizontal plane) and with the plane formed by the anterior superior iliac spine and the pubic symphysis aligned vertically (Ref 23). Osteotome was used to eliminate redundant intervertebral disk and other soft tissue and we made a platform for load test using self-curing denture acrylic on the top of the forth lumbar vertebra. The mounting hardware and pelves were attached superiorly to the load cell of a CSS-44000 electromechanical universal testing machine (Changchun Research Institute for Testing Machine Co., Ltd, Changchun, China) as shown in Fig. 1. Before the formal experiments, we performed

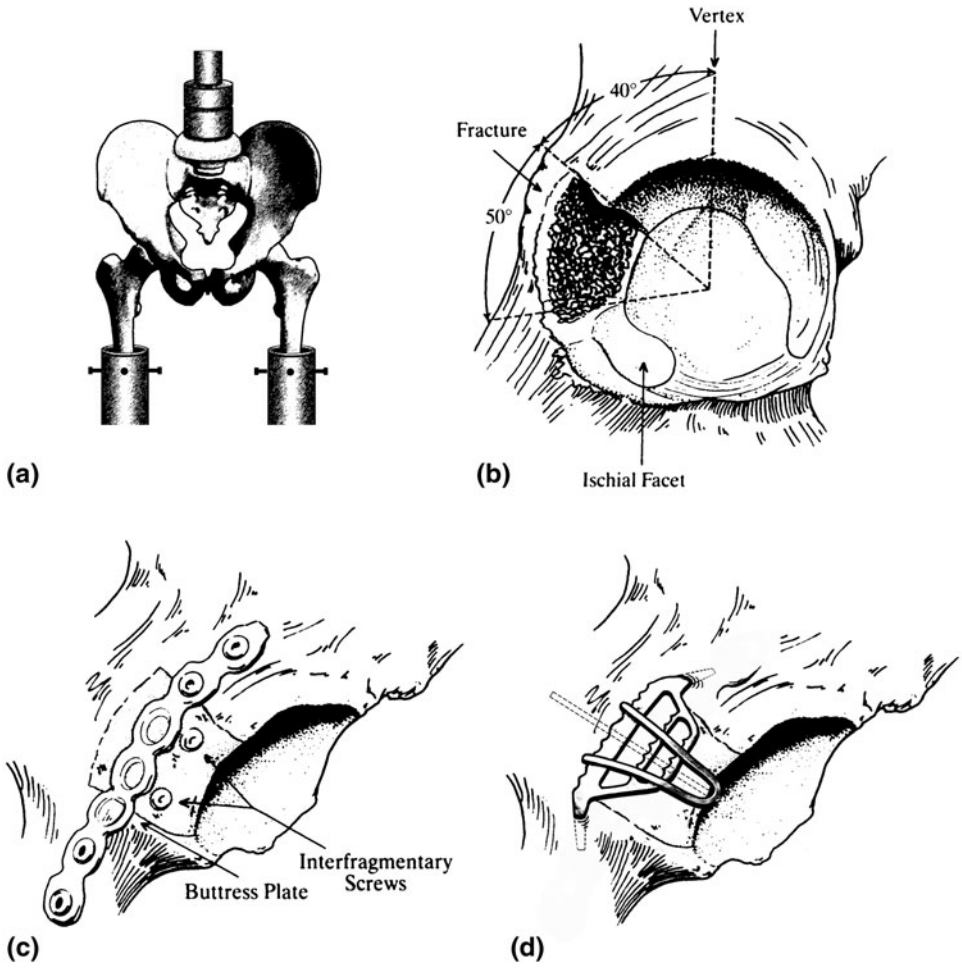

Fig. 1 (a) Illustration of the load cell and jig used to position the pelvis and femur. (b) Illustration of the simulated fracture of the posterior wall of the acetabulum. The fracture began 40° posterior to the acetabular vertex and extended another 50°. The simulated fracture created a defect of the entire width of the articular surface of the posterior wall with this 50° arc. The inferior portion of the articular surface of the posterior wall (the ischial facet) remained intact. (c) Illustration of the repair of the fracture with interfragmentary screws and plate. (d) Illustration of the repair of the fracture with ATMFS

preliminary adjustment for three times according to the manufacture's instructions to eliminate the gap between testing machine and loaded specimen. During testing, the pelves were placed under loads that ranged from 0 to 4000 N within 2 min and the maximum loads were maintained for 2 min. No load to failure testing was performed.

2.2 Joint Contact Area and Pressure Measurement

Prior to testing, the joint was disarticulated and the capsule, labrum, and transverse acetabular ligament were resected. The capsule is excised as the use of pressure sensitive Fuji film requires disarticulation of the femoral head to apply the Fuji film into the curved surface of the femoral head between two latex layers and avoid minimize technique-related artifact on the film. In previous works, Konrath et al. (Ref 24) have explored the effects of resection of the labrum on hip loading using similar techniques. Removal of the labrum did not alter the recorded hip joint load as compared with loading the hip with the labrum intact. With the labrum resected, the ability to identify the rim of the acetabular articular surface on the Fuji Film is improved.

The vertex of the acetabulum was identified, and 2.0 mm holes were drilled as reference points though the articular cartilage and underlying bone, centered between the acetabular fossa and rim, at points 30° on either side of the vertex (Ref 16). During subsequent joint loading, blunt probes were inserted though the holes to mark the pressure sensitive film to establish orientation of the film with respect to the acetabulum for later analysis. The anterior and posterior regions of the acetabulum were defined as those areas that lay anterior and posterior, respectively, to the superior region. The acetabular rim was also circumscribed onto the pressure sensitive film during loading with a blunt probe to identify its location during analysis.

Pressure patterns were recorded with the Fuji film (Fuji Prescale, low range; Fuji Photo Film, Tokyo, Japan). This low-range film, which is sensitive to pressures between 2.5 and 10.0 MPa, was selected on the basis of previous reports of hip-joint contact pressures (Ref 25). Pressure sensitive film sheets were cut into identical 8-armed star shapes using a template created for each pelvis such that when the film was contoured to the femoral head with the center of the star shape located approximately over the fovea, complete coverage of the head was achieved without overlap of the arms. Before each load, the hip joint was distracted, the femoral head was covered with a latex barrier and the pressure sensitive film was placed onto the femoral head over the barrier and then covered with another latex barrier to keep the pressure sensitive film dry, but allowing the cartilage surface to be hydrated. These latex barriers are identical to those uses in previous works (Ref 14, 16, 23, 26, 27).

Each pelvis underwent loading under the four following conditions: (1) with the acetabulum intact; (2) following a creation posterior wall fracture defect with the fragment removed (Fig. 1b); (3) following reduction and fixation of the fracture fragment with reconstruction plate (Fig. 1c); and (4) following reduction and fixation with application of ATMFS (Fig. 1d). These four conditions will subsequently be referred to as intact, defect, fixation with plate, and fixation with ATMFS, respectively. All Fuji film recordings were analyzed for each experimental condition and an average of these data was calculated to represent the data for each experimental condition.

Each pelvis first underwent loading with pressure and contact area measurements with the acetabular wall intact. The simulated fracture of the posterior wall began at 40° posterior to the acetabular vertex along the rim of the acetabulum and continued along the arc of the posterior rim to 90° posterior to the vertex. The fragment extended medially to include 50% of the width of the retroacetabular surface, greater sciatic notch, and the entire width of the articular surface throughout the 50° arc was removed. The inferior portion of the posterior articular surface, which we refer to as the ischial facet, remained intact. The fracture of the posterior wall was made with the use of holes drilled to the subchondral bone but not through the articular cartilage. The drill-holes were connected with an osteotome to create a realistic fracture in the articular surface as described by Olson et al. (Ref 23). The specimen was then loaded as above and pressure and contact area measurements were performed with the fragment removed.

The fragment was reduced and fixed by Shuo-Gui Xu, an experienced surgeon, with a contoured 8-hole small fragment reconstruction plate and small-fragment screws (Weigao Orthopedic Device Co., Limited, Shandong, China). The fixation of the posterior wall accomplished by contouring the posterior wall plate to the intact bone before the posterior wall defect was created. Two interfragmentary screws were inserted through the posterior part of the fragment but outside the plate. All reductions were anatomical. There were small gaps in the interface between the fragment and intact bone that were less than 1 mm.

When in use, the ATMFS should first be placed in cold water of 0-4 °C to allow the pseudoplastic deformation of the NiTi alloy in martensite state. Then the arm should be unfolded using needle forceps, and a hole should be drilled to the intended fixing position, around the two sides of the fracture point, with the middle part of the arm aiming at the fracture fragment, see Fig. 1d. After the fracture sites are reduced, ATMFS should be implanted and reheated in warm (40-50 °C) water, to return to the austenite state with the appropriate mechanical behavior. The memory alloy creates three-dimensional stereo fixation by maintaining the bone block, after the transition took place by heating.

2.3 Analysis

Pressure and contact area were measured by FPD-301 pressure densitometer and FPD-302 pressure reader especially designed for the analysis of Fuji pressure-sensitive film. Film density values were read by FPD-301 pressure densitometer and we input these values into FPD-302 pressure reader. The microcomputer in FPD-302 pressure reader converted density values to pressure and printed them automatically. We randomly selected 15 points in each region on the film, the mean value of 15 points was named the mean pressure, and the maximum one was peak pressure. When contact area was measured, digitizing was conducted with a scanner (HP Scanjet G4010, Beijing, China). The calculation of contact area was performed by AutoCAD2004 software (Autodesk Co., Ltd., New York, USA). When the pressure-sensitive film was scanned, we simultaneously put a scale for the adjustment of image.

The mean and peak contact stresses, as well as contact area was determined for three anatomic regions. Articular load was determined by the product of mean contact stress and contact area. For data analysis the parameters measured from the Fuji film were averaged for each experimental condition for each

pelvis tested. For each of 6 hip joints, four experimental conditions (intact, defect, fixed with plate, and fixed with ATMFS) in three regions (anterior, posterior, and superior) were assessed for four outcome measures (MPa max, MPa mean, average area, and load). Two separate film patterns were recorded for each hip in each experimental condition. The repeat patterns were evaluated qualitatively for consistency at the time of the test, any pair that had obvious disagreement was rejected and the test was repeated. All measurements represent the mean of the two accepted repeat patterns. The paired *t* test was used to assess the significance of the differences between conditions separately for each region. Initially, all conditions were considered together; subsequently the tests were carried out separately for each pair of conditions, simultaneously for each region and then separately for each region. An alpha-level of 0.05 was used for each test for testing the significance.

3. Results

In all specimens, two recordings of each experimental condition were made. None of the specimens required a third recording. The averaged data from the two recordings of each experimental condition was used for data analysis. The results of contact pressure, area, and load are summarized in Table 1.

3.1 Contact Area

The distribution of contact area was approximately equal among the anterior, superior, and posterior regions, see Fig. 2. The fracture of the posterior wall caused a significant ($P = 0.005$) decrease in the total acetabular contact area and a redistribution of contact within the acetabulum (Fig. 2). The mean contact area changes were significant lower in all the three regions, with decreased contact area on the anterior ($P = 0.007$) and posterior ($P = 0.004$) walls, whereas the mean contact area increased on the superior aspect ($P = 0.04$).

Anatomical reduction and fixation of the fragment of the posterior wall with reconstruction plate restored the total contact area but did not restore the distribution of contact within the acetabulum to that of the intact condition. The total mean contact area was not different from the intact condition. The distributions of contact area to the anterior and posterior walls were not significantly different from the intact condition ($P = 0.08$ and 0.09, respectively), but the superior aspect contact area remained elevated ($P = 0.045$).

Following anatomical reduction and fixation of the fragment of the posterior wall with ATMFS, the distribution of contact

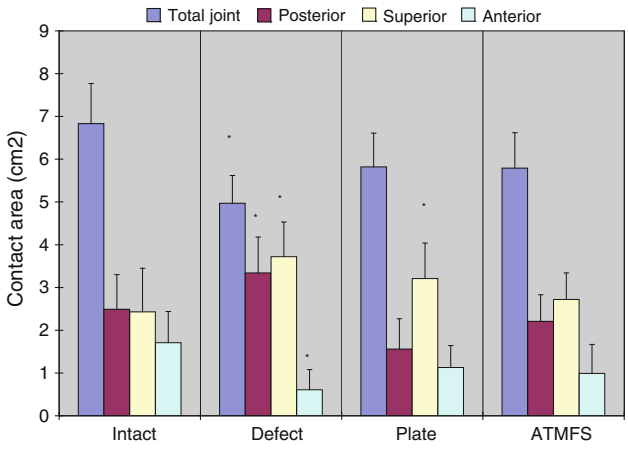

Fig. 2 The contact area. Graphs of the variations in the tested parameters for the four testing condition. The mean values and standard deviations for the six specimens are shown. An asterisk indicates a value that is significantly different ($P < 0.05$) from the corresponding value for the intact joint

Table 1 Contact area, contact pressures, and calculated load observed in the anterior, superior, posterior walls of acetabulum for the four tested conditions ($n = 7$)

	Intact		Defect		Plate		ATMFS	
	Mean	SD	Mean	SD	Mean	SD	Mean	SD
Anterior								
Contact area, cm^2	1.71	0.76	0.61	0.47	1.13	0.51	0.99	0.68
Mean, Mpa	3.21	0.31	2.93	0.26	3.02	0.24	2.99	0.35
Peak, Mpa	7.46	2.01	6.86	0.84	6.4	0.91	6.35	0.83
Load, N	550	314	179	105	321	92	286	154
Superior								
Contact area, cm^2	2.43	1.02	3.72	0.81	3.21	0.83	2.72	0.62
Mean, Mpa	3.02	0.82	3.99	0.54	3.68	0.34	3.54	0.49
Peak, Mpa	7.18	1.17	8.57	0.67	7.34	0.71	7.18	0.81
Load, N	748	382	1485	279	1545	533	964	298
Posterior								
Contact area, cm^2	2.49	0.94	0.81	0.65	1.56	0.71	2.21	0.62
Mean, Mpa	3.12	0.77	3.34	0.84	3.41	0.92	3.56	1.37
Peak, Mpa	6.24	0.84	7.49	1.35	7.68	1.62	7.6	1.58
Load, N	789	411	272	152	542	248	789	336
Total joint								
Contact area, cm^2	6.83	0.94	4.97	0.65	5.82	0.79	5.79	0.83
Mean, Mpa	3.11	0.57	3.73	0.82	3.46	0.97	3.63	0.62
Peak, Mpa	6.85	1.34	6.99	1.49	7.22	1.63	7.19	1.42
Load, N	2134	401	1864	322	2017	319	2102	402

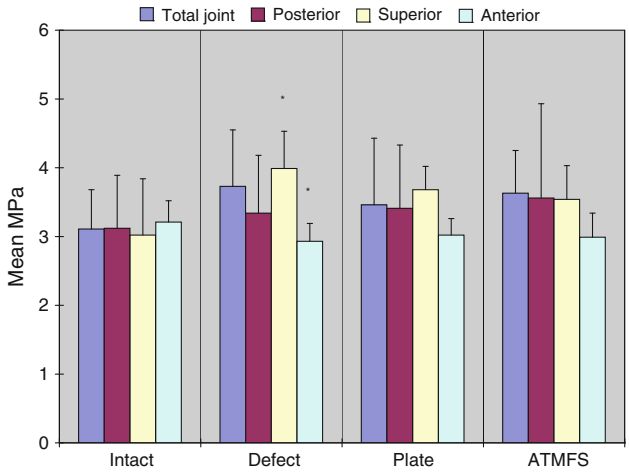

Fig. 3 The mean contact pressure. There was significantly greater ($P < 0.05$) mean pressure on the superior aspect and lower ($P < 0.05$) mean pressure on the anterior aspect of the acetabulum in the defect condition

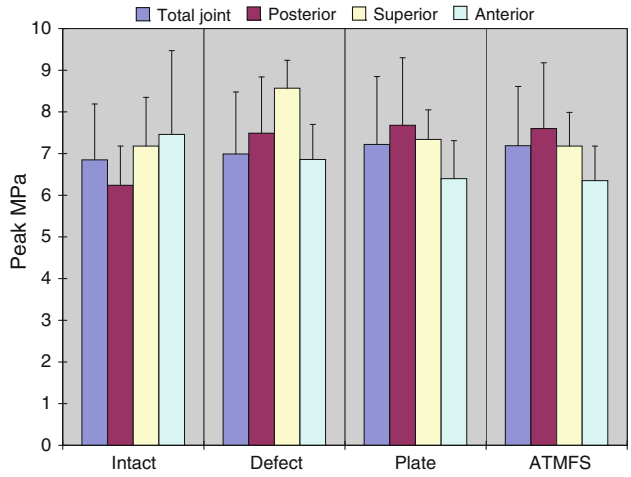

Fig. 4 The peak pressure. The peak pressure magnitudes were roughly similar among all tested conditions and among the distribution for the three anatomic regions

area was no longer statistically different from the intact condition. The total contact area following ATMFS application was not statistically different from the result with application of reconstruction plate but the distributions of contact area to superior walls were significantly different from the condition of application of reconstruction plate ($P = 0.048$).

3.2 Contact Pressure

There were significant changes in the mean pressure in the anterior and superior aspect of the intact acetabulum in response to the defect group (Fig. 3). Following a posterior wall fracture defect, decreased mean pressure on the anterior ($P = 0.009$) wall and increased mean pressure on the superior aspect ($P = 0.03$) were observed. The overall mean pressure and the distribution for the three anatomic regions were roughly similar after anatomical reduction and fixation of the fragment of the posterior wall with the application of reconstruction plate or ATMFS.

The peak pressure magnitudes were roughly similar among all tested conditions and among the distribution for the three anatomic regions (Fig. 4). The overall peak pressures were roughly similar for each condition.

3.3 Load Distribution

As the mean contact pressures are roughly constant, the calculated mean contact load (the product of mean contact area and mean contact pressure) had a pattern similar to that of the contact area (Fig. 5). Following a posterior wall defect the load decreased in the anterior and posterior regions ($P = 0.006$ and 0.008, respectively), and increased in the superior region ($P = 0.009$).

After fracture fixation with reconstruction plate the loads in the anterior and superior regions were significantly different from the intact condition, with anterior and superior walls ($P = 0.03$ and 0.04, respectively). However, the load in the posterior region was not significantly different from the intact condition ($P = 0.35$). The loads of the superior and anterior aspects are significantly different from the intact condition in both the defect and the plate fixed conditions. After fixation with ATMFS, the loads in the superior and posterior regions

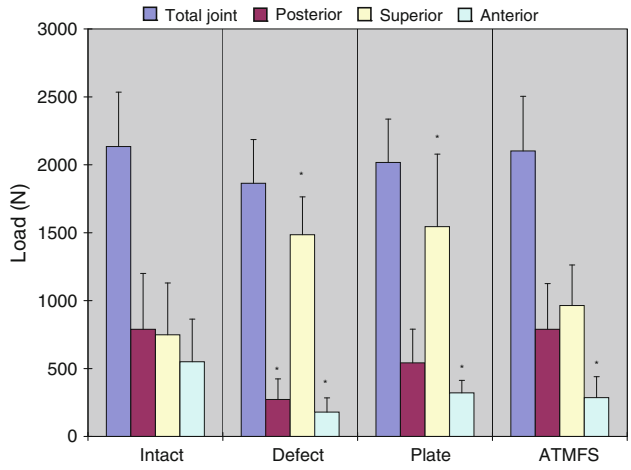

Fig. 5 The distribution of load. Load distribution is not improved (returned toward normal) in ATMFS fixed condition. The loads seen in the superior and anterior aspects are significantly different from the intact condition in both the defect and plate fixed conditions

were not significantly different from the intact condition, ($P = 0.45$ and 0.85, respectively). However, the load in the anterior region decreased when compared to the intact condition ($P = 0.045$).

4. Discussion

The results of this study demonstrate that fractures of the posterior wall of the acetabulum significantly alter the patterns of contact area and pressure in the hip joint during double-limb stance and these parameters, which were statistically different from the normal state, returned to statistically similar levels following fixation with reconstruction plate or ATMFS. After the fracture, the total articular contact area was decreased by 1.86 cm^2. Within the acetabulum, the contact area was simultaneously decreased on the anterior wall (by 1.1 cm^2) and the posterior wall (by 1.29 cm^2) and was increase on the

superior aspect of the acetabulum (by 0.85 cm^2). The mean pressure on the superior aspect of the acetabulum increased as well. Parameters of contact area and load distribution, which were statistically different from the normal state following creation of a posterior wall defect, returned to statistically similar levels following fixation with plate or ATMFS. The total contact area following ATMFS application was not statistically different from the result with application of reconstruction plate, but only the distributions of contact area to superior walls were significantly different from the condition of application of reconstruction plate ($P = 0.045$). Following the fixation with ATMFS, the load seen at the superior region of the actabulum (964 N) was similar to fixation with reconstruction plate and was not different from intact state ($P = 0.45$). ATMFS does not have biomechanical advantages over plate but these results above suggest that the use of reconstruction plate or ATMFS in this investigation moved the observed loading characteristics toward the normal condition.

The material of fixation system is expected to have a modulus equivalent to that of bone. The bone modulus varies in the magnitude from 4 to 30 GPa depending on the type of the bone and direction of measurement (Ref 28). The current implant materials, such as stainless steel which have higher stiffness than bone, prevent the needed stress being transferred to adjacent bone, resulting in bone resorption around the implant and consequently to implant loosening. This biomechanical incompatibility that leads to death of bone cells is called as ''stress shielding effect'' (Ref 29). Thus a material with excellent combination of high strength and low modulus closer to bone has to be used for implantation to avoid loosening of implants and higher service period to avoid revision surgery. Ni-Ti alloy has lower elastic modulus and is close to the bones' elasticity modulus, thus Ni-Ti alloy has better stress compliance with the bone and the resorption action which can lead to failed fixation hardly occur when the bones are under load (Ref 30, 31). From this perspective, a fixation system made of Ni-Ti alloy would be advantageous.

Our interpretation of the changes in the mechanics of the hip joint after a fracture and the success of anatomical operative repair to restore normal loading is based on the concept of the hip as an incongruous joint in which the femoral head is somewhat larger in diameter than the unloaded acetabulum (Ref 16). The contact at low loads is anterior and posterior, with the superior region unloaded. At loads of more than approximately one-quarter to one-half body weight, the femoral head makes contact with the superior portion of the acetabulum. At higher loads, such as those that occur during walking, the contact zone and pressure are spread evenly over the surface of the acetabulum by a combination of bone and cartilage deformation. During this process, the femoral head expands the joint by forcing the anterior and posterior walls apart, and peripheral contact pressures result.

Every fracture of the acetabulum alters the load distribution acutely, resulting in increased loading in the superior aspect of the acetabulum (Ref 13, 14, 16, 26, 27, 32-34). Olson demonstrated a similar effect when the acetabulum was explanted from the intact pelvic ring (Ref 23). They hypothesized that the peripheral loading seen in the intact pelvis results from bending or deformation of the acetabulum about the femoral head during loading. Explanting the acetabulum from the pelvis had the effect of eliminating this behavior during load resulting in load that occurred primarily on the superior acetabulum. Fractures of the acetabulum in cadaveric models appear to behave in a biomechanically similar manner. We observed an even distribution of all parameters (contact area, mean and maximum pressure, and contact force) in the intact joint at a load of 4000 newtons and a clear decrease in peripheral contact after simulated fracture of the posterior wall. With the circumferential congruity of the acetabulum disrupted, there is little resistance to expansion and the femoral head makes superior contact without the development of normal peripheral contact force. Decreased peripheral contact also explains the increase in contact force within the superior aspect of the acetabulum of the fractured joint. Success of fixation to restore normal mechanics of the joint indicates adequate stiffness of, or adequate load transfer to, the reconstruction hardware.

The experimental protocol used in this study has an advantage compared with previous biomechanical studies of normal hip joints. By leaving the pelvic ring intact for mechanical testing, more normal deformations of the acetabulum can be expected with loading than would be the case when the ilium is rigidly embedded in plastic. Because the femur and pelvis are mounted and aligned with the ligamentous structures and capsule intact, anatomical positioning can be ensured. Thereafter, the specimen can be returned repeatedly to this alignment even after the joint has been disarticulated.

The advantage of pressure-sensitive film is that it can be used to measure joint-contact areas and pressures simultaneously. Other methods that have been employed in investigations of the hip joint can be used to measure contact area but not pressure (dye studies and castings) or to measure pressure locally but not globally (piezoelectric transducers and mechanical transducers) (Ref 22, 34). The dye transfer basis of the film and the need to digitize and process image data can lead to measurements that are more variable than those made with transducer-based techniques. Pressures measured are in a range, not continuously, to a maximum limiting value. Low-range film, for example, is most accurate between 2.5 and 10.0 MPa. By thresholding, we specially excluded any signal of less than 2.5 MPa. Accurate measurements also require application and maintenance of load during a period of time that is substantially longer than the stance phase of gait. Therefore, slow loading was chosen (4000 N in 2 min). Creep deformation of cartilage during the loading period could alter the area and pressure measurements made by the film (Ref 35, 36).

The restoration of normal joint contact area and load distribution may help prevent the development of posttraumatic arthritis. Altered joint loading has been postulated as one mechanism that may result in posttraumatic osteoarthritis (Ref 14, 18). In this investigation, we documented changes in hip joint loading following a simulated posterior wall fracture. The guiding hypothesis is that increased stresses within the cartilage exceed the capacity of the tissue to adapt, initiating a cascade of degenerative changes that ultimately leads to the development of arthritis in the joint. Evidence exists that increased loads, especially in the superior region of the acetabulum, do lead to degenerative arthrosis (Ref 32, 37). These changes are restored toward the intact condition following open reduction and internal fixation (ORIF) with reconstruction plate or ATMFS.

Alternatively, instability has also been suggested as a mechanism leading to the development of osteoarthritis. In highly congruent articulations, such as the hip joint, residual articular displacement is often associated with subluxation incongruency, a sign of instability after fracture. Improving stability of fixation with shape memory alloy may also help

address the issue of posttraumatic arthritis. Although both ATMFS and plate can be used to fix the fracture of posterior wall of acetabulum, long-term stability following the use of ATMFS applied as an internal fixation device is unknown.

We observed increases of 32.1% in mean pressure and 19.4% in maximum pressure on the superior aspect of the acetabulum after a fracture of the posterior wall. Failure to repair or inaccurate reduction of such a fracture might lead to later degenerative changes, as has been shown in previous clinical studies (Ref 17, 38). The satisfactory long-term results after anatomical repair demonstrated by some authors (Ref 12, 39, 40) suggest that healing of the fracture may restore the mechanics of the joint.

As with all studies, ours has weaknesses. The sample population limits our ability to achieve statistical power in some instances. In addition, this study was performed using formalin-preserved specimens and we may have introduced bias, as human fresh frozen cadaveric pelvis tend to perform more favorably regarding biomechanical testing.

5. Conclusion

The results of this study suggest that reconstruction plate and ATMFS used as a internal fixation device for posterior wall fracture of acetabulum resulted in contact area and load distribution parameters that were observed to be at levels similar to the intact condition. More work is needed to understand the potential clinical significance of these findings.

Acknowledgments

This research was supported by a grant from National Natural Science Foundation of China (No. 30872640/C160705) & Nano Project of Science and Technology Commission of Shanghai Municipality (No. 1052nm03100).

References

1. W.J. Buehler and F.E. Wang, A Summery of Recent Research on Nitinol Alloys, Their Potential Application in Ocean Engineering, *Ocean Eng.*, 1968, **1**, p 105–120
2. Y. Oshida and S. Miyazaki, Corrosion and Biocompatibility of Shape Memory Alloys, *Corros. Eng.*, 1991, **40**, p 1009–1025
3. J.O. Sanders, A.E. Sanders, R. More, and R.B. Ashman, A Preliminary Investigation of Shape Memory Alloys in the Surgical Correction of Scoliosis, *Spine*, 1993, **18**, p 1640–1646
4. A. Kapanen, J. Ryhanen, A. Danilov, and J. Tuukkanen, Effect of Nickel-Titanium Shape Memory Metal Alloy on Bone Formation, *Biomaterials*, 2001, **22**, p 2475–2480
5. M. Assad, N. Lemieux, and C.H. Rivard, Comparative in Vitro Biocompatibility of Nickel-Titanium, Pure Nickel, Pure Titanium, and Stainless Steel: Genotoxicity and Atomic Absorption Evaluation, *Biomed. Mater. Eng.*, 1999, **9**, p 1–12
6. D.S. Levi, N. Kusnezov, and G.P. Carman, Smart Materials Applications for Pediatric Cardiovascular Devices, *Pediatr. Res.*, 2008, **63**, p 552–558
7. K.T. Oh, U.H. Joo, G.H. Park, C.J. Hwang, and K.N. Kim, Effect of Silver Addition on the Properties of Nickel-Titanium Alloys for Dental Application, *J. Biomed. Mater. Res. B*, 2006, **76**, p 306–314
8. D.C. Templeman, S. Olson, B.R. Moed, P. Duwelius, and J.M. Matta, Surgical Treatment of Acetabular Fractures, *Instr. Course Lect.*, 1999, **48**, p 481–496
9. J.K. Yu, F.Y. Chiu, C.K. Feng et al., Surgical Treatment of Displaced Fractures of Posterior Column and Posterior Wall of the Acetabulum, *Injury*, 2004, **35**, p 700–766
10. B.R. Moed, E. Seann, C. Willson et al., Results of Operative Treatment of Fractures of the Posterior Wall of the Acetabulum, *J. Bone Joint Surg. Am.*, 2002, **84**, p 752–758
11. P.V. Giannoudis, C. Tzioupis, and B.R. Moed, Two-Level Reconstruction of Comminuted Posterior-Wall Fractures of the Acetabulum, *J. Bone Joint Surg. Br.*, 2007, **89**, p 503–509
12. G. Petsatodis, P. Antonarakos, B. Chalidis, P. Papadopoulos, J. Christoforidis, J. Pournaras et al., Surgically Treated Acetabular Fractures via a Single Posterior Approach with a Follow-Up of 2–10 Years, *Injury*, 2007, **38**, p 334–343
13. G.A. Konrath, A.J. Hamel, N.A. Sharkey, B. Bay, and S.A. Olson, Biomechanical Evaluation of a Low Anterior Wall Fracture: Correlation with the CT Subchondral Arc, *J. Orthop. Trauma*, 1998, **12**, p 152–158
14. S.A. Olson, B.K. Bay, and A. Hamel, Biomechanics of the Hip Joint and the Effects of Fracture of the Acetabulum, *Clin. Orthop. Relat. Res.*, 1997, **20**, p 92–104
15. J.A. Goulet, J.P. Rouleau, D.J. Mason, and S.A. Goldstein, Comminuted Fractures of the Posterior Wall of the Acetabulum, A Biomechanical Evaluation of Fixation Methods, *J. Bone Joint Surg. Am.*, 1994, **76**, p 1457–1463
16. S.A. Olson, B.K. Bay, M.W. Chapman, and N.A. Sharkey, Biomechanical Consequences of Fracture and Repair of the Posterior Wall of the Acetabulum, *J. Bone Joint Surg. Am.*, 1995, **77**, p 1184–1192
17. J.M. Matta, Fractures of the Acetabulum: Accuracy of Reduction and Clinical Results in Patients Managed Operatively Within Three Weeks After the Injury, *J. Bone Joint Surg. Am.*, 1996, **78**, p 1632–1645
18. N.A. Hadley, T.D. Brown, and S.L. Weinstein, The Effects of Contact Pressure Elevations and Aseptic Necrosis on the Long-Term Outcome of Congenital Hip Dislocation, *J. Orthop. Res.*, 1990, **8**, p 504–513
19. M. Geetha, A.K. Singh, R. Asokamani, and A.K. Gogia, Ti Based Biomaterials, the Ultimate Choice for Orthopaedic Implants—A Review, *Prog. Mater. Sci.*, 2009, **54**, p 397–425
20. C. Zhang, S. Xu, J. Wang, B. Yu, T. Hou, F. Ji et al., Design and Clinical Applications of Acetabular Tridimensional Memoryalloy-Fixation System, *Chin. J. Orthop.*, 2002, **22**, p 709–713
21. C. Zhang, S. Xu, W. Xu, H. Shen, J. Su, J. Wang et al., Application of Acetabular Tridimensional Memory Fixation System (ATMFS) to Treat Complex Acetabular Fractures and Its Clinical Significance, *Chin. J. Orthop. Trauma*, 2004, **6**, p 364–368
22. T. Sawaguchi, T.D. Brown, H.E. Rubash, and D.C. Mears, Stability of Acetabular Fractures After Internal Fixation. A Cadaveric Study, *Acta Orthop. Scand.*, 1984, **55**, p 601–605
23. S.A. Olson, M.W. Kadrmas, J.D. Hernandez, R.R. Glisson, and J.L. West, Augmentation of Posterior Wall Acetabular Fracture Fixation Using Calcium-Phosphate Cement: A Biomechanical Analysis, *J. Orthop. Trauma*, 2007, **21**, p 608–616
24. G.A. Konrath, A.J. Hamel, S.A. Olson, B. Bay, and N.A. Sharkey, The Role of the Acetabular Labrum and the Transverse Acetabular Ligament in Load Transmission in the Hip, *J. Bone Joint Surg. Am.*, 1998, **80**, p 1781–1788
25. N.Y. Afoke, P.D. Byers, and W.C. Hutton, Contact Pressures in the Human Hip Joint, *J. Bone Joint Surg. Br.*, 1987, **69**, p 536–541
26. D.J. Hak, A.J. Hamel, B.K. Bay, N.A. Sharkey, and S.A. Olson, Consequences of Transverse Acetabular Fracture Malreduction on Load Transmission Across the Hip Joint, *J. Orthop. Trauma*, 1998, **12**, p 90–100
27. S.A. Olson, B.K. Bay, A.N. Pollak, N.A. Sharkey, and T. Lee, The Effect of Variable Size Posterior Wall Acetabular Fractures on Contact Characteristics of the Hip Joint, *J. Orthop. Trauma*, 1996, **10**, p 395–402
28. J. Lawrence Katz, Anisotropy of Yong's modulus of bone, *Nature*, 1980, **283**, p 106–107
29. T. Sawaguchi, T.D. Brown, H.E. Rubash, and D.C. Mears, Stability of Acetabular Fractures After Internal Fixation: A Cadaveric Study, *Acta Orthop. Scand.*, 1984, **55**, p 601–605
30. D.R. Summer, T.M. Turner, R. Igloria, R.M. Urban, and J.O. Galante, Functional Adaptation and Ingrowth of Bone Vary as a Function of Hip Implant Stiffness, *J. Biomech.*, 1998, **31**, p 909–917

31. A.K. Jorma, A.D. Ryhanen, and T. Juha, Effect of Nickel-Titanium Shape Memory Metal Alloy on Bone Formation, *Biomaterials*, 2001, **222**, p 2475
32. G.I. Im, Y.W. Shin, and Y.J. Song, Fractures to the Posterior Wall of the Acetabulum Managed With Screws Alone, *J. Trauma*, 2005, **58**, p 300–303
33. G.A. Konrath, A.J. Hamel, N.A. Sharkey, B.K. Bay, and S.A. Olson, Biomechanical Consequences of Anterior Column Fracture of the Acetabulum, *J. Orthop. Trauma*, 1998, **12**, p 547–552
34. B.J. Lankester, O. Sabri, S. Gheduzzi, J.D. Stoney, A.W. Miles, G.C. Bannister et al., In Vitro Pressurization of the Acetabular Cement Mantle: The Effect of a Flange, *J. Arthroplasty*, 2007, **22**, p 738–744
35. M.A. Adams, A.J. Kerin, L.S. Bhatia, G. Chakrabarty, and P. Dolan, Experimental Determination of Stress Distributions in Articular Cartilage Before and After Sustained Loading, *Clin. Biomech. (Bristol Avon)*, 1999, **14**, p 88–96
36. M. Oka, K. Ushio, P. Kumar, K. Ikeuchi, S.H. Hyon, T. Nakamura et al., Development of Artificial Articular Cartilage, *Proc. Inst. Mech. Eng. H*, 2000, **214**, p 59–68
37. B.D. Furman, S.A. Olson, and F. Guilak, The Development of Posttraumatic Arthritis After Articular Fracture, *J. Orthop. Trauma*, 2006, **20**, p 719–725
38. P. Tornetta, III, Displaced acetabular fractures: indications for operative and nonoperative management, *J. Am. Acad. Orthop. Surg.*, 2001, **9**, p 18–28
39. P.V. Giannoudis, M.R. Grotz, C. Papakostidis, and H. Dinopoulos, Operative Treatment of Displaced Fractures of the Acetabulum: A Meta-Analysis, *J. Bone Joint Surg. Br.*, 2005, **87**, p 2–9
40. J.M. Matta, Operative Treatment of Acetabular Fractures Through the Ilioinguinal Approach: A 10-Year Perspective, *J. Orthop. Trauma*, 2006, **20**, p 20–29